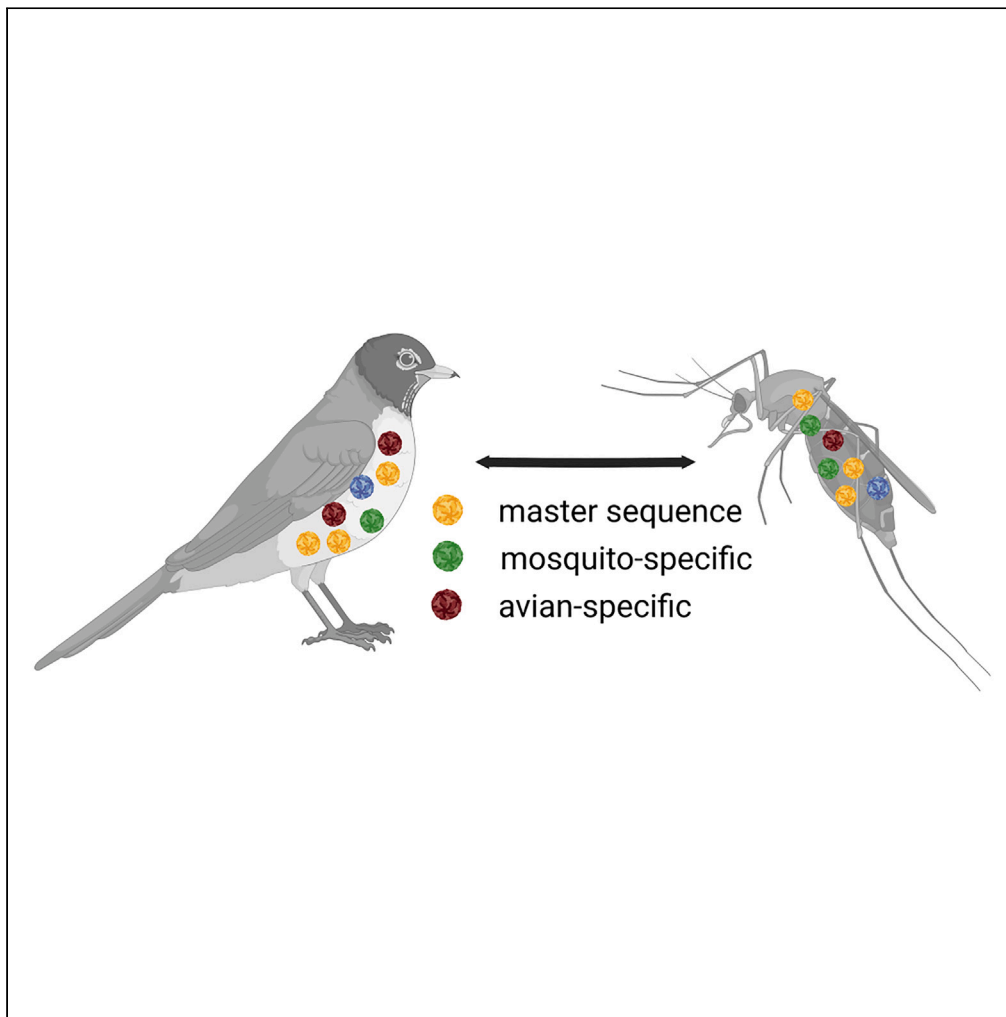


Article

Maintenance of a host-specific minority mutation in the West Nile virus NS3



Haley S. Caldwell,
Lili Kuo, Janice D.
Pata, ..., Taylor A.
Nolen, Craig E.
Cameron,
Alexander T. Ciota

alexander.ciota@health.ny.gov

Highlights

WNV minority substitutions including NS3 P319L are maintained in nature

NS3 P319L demonstrates host-specific fitness and temperature sensitivity *in vitro*

NS3 P319L is attenuated in vertebrate hosts and more transmissible by *Cx. pipiens*

Temperature-sensitive ATPase activity is consistent with host-specific phenotypes

Caldwell et al., iScience 26, 107468
August 18, 2023 © 2023 The Author(s).
<https://doi.org/10.1016/j.isci.2023.107468>

Article

Maintenance of a host-specific minority mutation in the West Nile virus NS3

Haley S. Caldwell,^{1,2} Lili Kuo,¹ Janice D. Pata,^{2,3} Alan P. Dupuis II,¹ Jamie J. Arnold,⁴ Calvin Yeager,⁴ Jessica Stout,¹ Cheri A. Koetzner,¹ Anne F. Payne,¹ Sean M. Bialosuknia,¹ Elyse M. Banker,¹ Taylor A. Nolen,¹ Craig E. Cameron,⁴ and Alexander T. Ciota^{1,2,5,*}

SUMMARY

West Nile virus (WNV), the most prevalent arthropod-borne virus (arbovirus) in the United States, is maintained in a cycle between *Culex* spp. mosquitoes and birds. Arboviruses exist within hosts and vectors as a diverse set of closely related genotypes. In theory, this genetic diversity can facilitate adaptation to distinct environments during host cycling, yet host-specific fitness of minority genotypes has not been assessed. Utilizing WNV deep-sequencing data, we previously identified a naturally occurring, mosquito-biased substitution, NS3 P319L. Using both cell culture and experimental infection in natural hosts, we demonstrated that this substitution confers attenuation in vertebrate hosts and increased transmissibility by mosquitoes. Biochemical assays demonstrated temperature-sensitive ATPase activity consistent with host-specific phenotypes. Together these data confirm the maintenance of host-specific minority variants in arbovirus mutant swarms, suggest a unique role for NS3 in viral fitness, and demonstrate that intrahost sequence data can inform mechanisms of host-specific adaptation.

INTRODUCTION

West Nile virus (WNV; *Flaviviridae*, *Flavivirus*) is the most geographically widespread arthropod-borne virus (arbovirus) globally and the most prevalent arbovirus in the United States.^{1,2} Known to primarily cause West Nile fever and be associated with neurological complications in approximately 1% of infections, WNV is maintained in an enzootic cycle between birds and *Culex* spp. mosquitoes, with humans and horses acting as notable dead-end hosts.³ Mosquito and avian hosts have highly distinct target cells, immune systems, internal temperatures, and tissue barriers.^{4,5} How arboviruses like WNV can fluctuate between these divergent environments efficiently while maintaining fitness is not fully understood, but studies on viral diversity suggest a role for mutant swarm plasticity and quasispecies structure.⁶

Genome diversity is generated as a result of error-prone replication of WNV and other arboviruses. High error rates among RNA-dependent RNA polymerases (RdRps), on the order of 1 mutation per genome, result from the lack of proofreading due to the absence of a 3' to 5' exonuclease present in eukaryotic and coronavirus polymerases.^{7,8} These high error rates result in diverse viral swarms which are postulated to facilitate maintenance of viral fitness, virulence, tissue tropism, and host adaptation.^{9–18}

Despite the lack of proofreading, fidelity (the inherent error rate of the polymerase) can be perturbed by amino acid substitutions resulting in structural modifications to the replication complex. Multiple studies have examined the importance of viral diversity of flaviviruses using fidelity mutants, which either expand (low fidelity) or reduce (high fidelity) the resultant viral diversity. Previously identified WNV high- and low-fidelity variants were found to possess mutations in the RdRp and the methyltransferase, respectively, and to be less infectious to mosquitoes, while closely related St. Louis encephalitis virus (SLEV) high-fidelity variants were shown to be attenuated in mosquito cells.^{19,20} Importantly, *in vitro* passage studies have additionally demonstrated that perturbing WNV fidelity decreases the capacity for maintenance during host cell alteration.²¹

We previously examined naturally occurring diversity of WNV and identified non-synonymous minority substitutions that occurred preferentially in mosquito or avian hosts and were retained through time without

¹The Arbovirus Laboratory, Wadsworth Center, New York State Department of Health, Slingerlands, NY 12159, USA

²Department of Biomedical Sciences, State University of New York at Albany, School of Public Health, Rensselaer, NY 12144, USA

³Wadsworth Center, New York State Department of Health, Albany, NY 12208, USA

⁴Department of Microbiology and Immunology, University of North Carolina School of Medicine, Chapel Hill, NC 27599, USA

⁵Lead contact

*Correspondence: alexander.ciota@health.ny.gov

<https://doi.org/10.1016/j.isci.2023.107468>



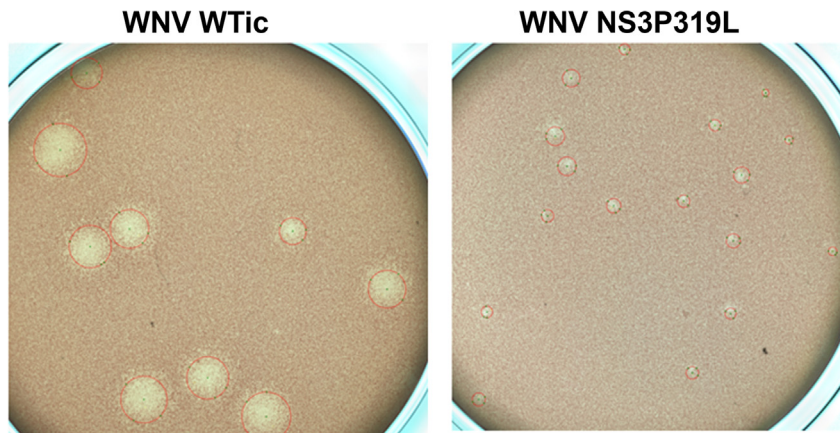


Figure 1. Decreased plaque size of West Nile virus NS3 P319L in mammalian cells

Representative images of a well following plaque titration of WNV WTic and NS3 P319L on Vero cell culture are shown. Red circles indicate the visualized plaque size used to calculate area for each plaque. Significantly smaller plaques were measured for WNV NS3 P319L (unpaired t test**** $p < 0.0001$).

fixation in consensus sequences.²² Minority variants of WNV identified through sequential passage have been shown to be critical for viral fitness in mosquito cells.¹⁶ Therefore, we hypothesized that variants with host-specific advantages and attenuation in alternate hosts are maintained during WNV cycling in nature, fluctuating in prevalence due to disparate selective pressures and fostering transient host-specific adaptation. Identifying and characterizing these mutations could facilitate a better understanding of the role of the viral swarm in host cycling and provide targets to probe the mechanisms of host-specific fitness. The majority of host-biased minority mutations have been identified within genes coding for the subunits of the WNV replicase demonstrating catalytic activity (NS3 and NS5), which drive viral replication and genome diversity.^{9,22} The WNV NS3 gene, which has previously been implicated in mosquito and avian competence,²³ encodes a C-terminal helicase and an N-terminal serine protease.²⁴ In order to test the hypothesis that host-specific WNV NS3 mutants exist as minority variants, and to further elucidate the role of the WNV NS3 in viral fitness in mosquitoes, we characterized the influence of a naturally occurring, mosquito-biased amino acid substitution, P1825L (NS3 P319L) in viral fitness and examined the mechanistic basis for phenotypic variability associated with this substitution. Our results confirm the maintenance of host-specific WNV variants in nature and shed light on the capacity of NS3 to contribute to viral fitness in divergent hosts.

RESULTS

Selection of the mosquito-biased substitution NS3 P319L

The mutation from cytosine to uracil at position 5570 of the WNV genome, resulting in a proline to leucine substitution at residue 1825 (NS3 319), was selected for characterization because it was shown to be maintained exclusively in minority sequences, identified over multiple years, and mosquito biased.²² Specifically, NS3 P319L was first identified in minority sequencing reads from a 2003 WNV isolate from *Culex* mosquitoes and subsequently identified in all but one year (2004) through 2014. In total, 40/89 (44.9%) of WNV isolates from *Culex* mosquitoes for which minority sequence data were previously obtained were found to possess this substitution at levels $>2.0\%$ in the intrahost population. Conversely, of the 139 WNV isolates from birds sequenced and analyzed from that period, none possessed NS3 P319L in minority reads at levels $>2.0\%$. While a total of 7 non-synonymous mutations with a mosquito bias were previously identified, C5570U was the only mutation that was not found in any avian isolate.²² These data demonstrate a highly significant bias for NS3 P319L in mosquitoes (chi-squared, $p < 0.0001$).

Cell-specific attenuation and temperature dependence of WNV NS3 P319L

Initial plaque titration of WNV NS3 P319L revealed significant attenuation in mammalian (Vero) cells. This attenuation was indicated by plaque size, with NS3 P319L forming significantly smaller plaques than the wild-type (WT) infectious clone (WNV WTic; unpaired t test, $p < 0.0001$; Figure 1).

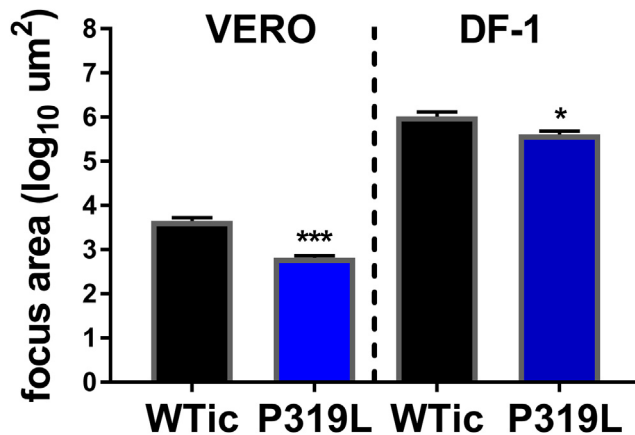


Figure 2. West Nile virus NS3 P319L is attenuated in mammalian and avian cells

Shown is the fluorescent focus area (mean \pm SEM, $n = 5-15$) of wild-type WNV (WTic) and WNV NS3 P319L in Vero (mammalian) and DF-1 (avian) cell lines. Significantly smaller foci were measured for WNV NS3 P319L in both cell lines (unpaired t test, *** $p < 0.0001$, * $p = 0.019$), yet the mean difference between WTic and P319L was significantly greater in Vero cells (unpaired t test, $p = 0.007$).

Because WNV does not form quantifiable plaques on avian cell culture, fluorescent focus assays (FFAs) were performed on Vero and DF-1 (avian) cell culture to determine if impaired cell-to-cell spread of WNV NS3 P319L was similar in mammalian and avian cells. Consistent with plaque results, WNV NS3 P319L formed significantly smaller foci in Vero cells (Figure 2; unpaired t test, $p < 0.0001$). FFA in avian cells also demonstrated attenuation (Figure 2; unpaired t test, $p = 0.0192$), yet the mean difference in foci area between WNV WTic and WNV NS3 P319L was greater in mammalian cell culture (unpaired t test, $p = 0.0007$).

Multi-step growth kinetics confirmed significant attenuation of WNV NS3 P319L in mammalian cell lines and modest attenuation in avian cell lines (Figure 3). In the mosquito cell line CxT, WNV NS3 P319L growth was statistically equivalent to WNV WTic (Figure 3A; paired t test, $p = 0.85$). However, in both Vero and human (A549) cells, WNV NS3 P319L growth was 1–3 log₁₀ plaque-forming units (pfu)/mL lower than WNV WTic (Figures 3B/D; paired t tests, $p < 0.01$). Additionally, deep sequencing of virus derived from the assay endpoint (120 h post-infection [HPI]) confirmed that the majority of the virus populations (82.8% and 96.8% for A549 and Vero, respectively) reverted to WT signature (NS3 P319; Table S1). In avian cells (DF-1), WNV NS3 P319L growth was also attenuated relative to WNV WTic (Figure 3C; paired t test, $p = 0.03$), yet differences in growth were significantly smaller than differences measured in mammalian cells (Figure 3F; ~ 0.5 log₁₀ pfu/ml; t test, $p < 0.05$). Consistent with this, deep sequencing of DF-1-derived virus demonstrated that just 2.3% of the population reverted to NS3 P319. No reversion was measured in mosquito cells (Table S1), and no additional mutations were identified in sequenced output viruses.

To further elucidate the role of temperature in attenuation of WNV NS3 P319L, growth kinetics were determined in Vero cell culture at 28°C. Results indicated attenuation relative to WNV WTic (Figure 3E; paired t test, $p = 0.01$), although to a lesser extent than measured at 37°C (Figure 3F; t test, $p < 0.05$). Together, these data indicate that both temperature and cell type contribute to attenuation of WNV NS3 P319L.

Increased transmissibility and decreased virulence of WNV P319L in *Culex pipiens*

Vector competence of *Cx. pipiens* for both WNV NS3 P319L and WNV WTic was evaluated to assess relative fitness *in vivo*. Significantly higher infection rates were measured for mosquitoes exposed to NS3 P319L at days 7, 14, and 21 post-feeding (Figure 4A; chi-squared, $p < 0.05$). Overall infection rates across days were 57.7% for WTic-exposed mosquitoes and 80.1% for NS3 P319L-exposed mosquitoes. Although mean viral loads in bodies (6.3 log₁₀ pfu/mosquito), and dissemination rates, were similar among virus strains, the proportion of exposed mosquitoes transmitting NS3 P319L was significantly higher than WTic at day 21 post-feeding (42.0% v. 16.1%; Figure 4A; chi-squared, $p = 0.015$).

Life-history studies were performed to determine strain-specific fitness effects in mosquitoes. Results demonstrated that exposure to WTic via blood feeding resulted in decreased mean longevity relative to

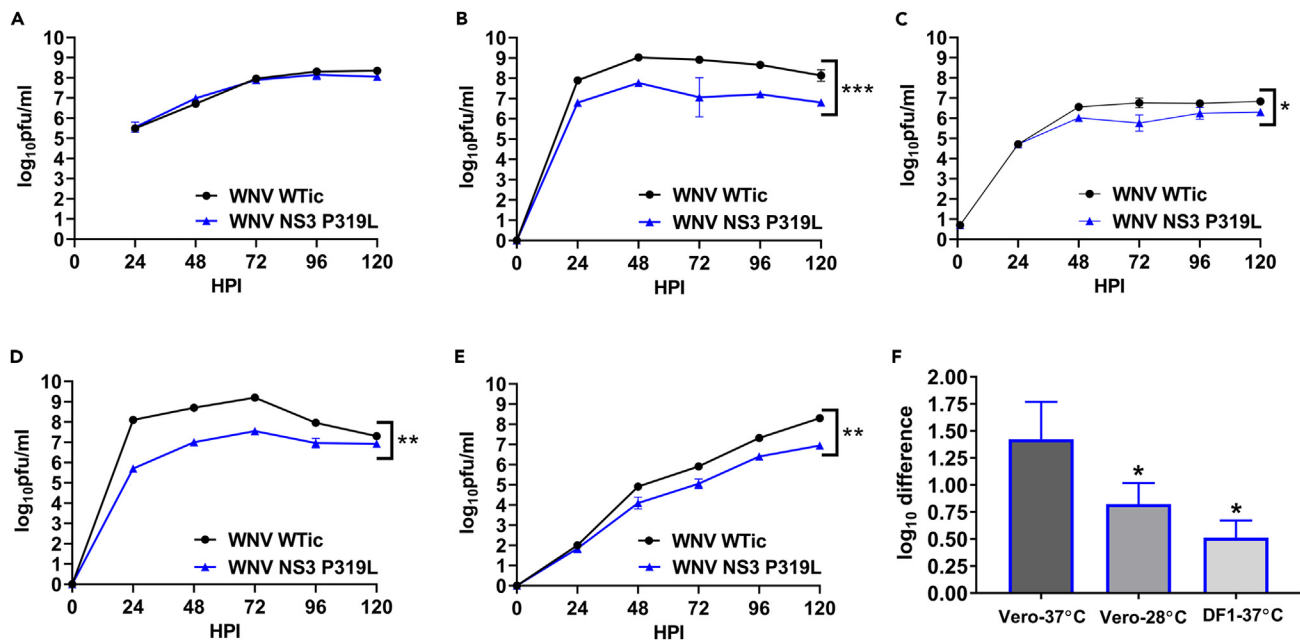


Figure 3. West Nile virus NS3 P319L demonstrates host-specific fitness and temperature sensitivity *in vitro*

(A–E) Growth kinetics of WNV NS3 P319L were compared to WNV WTic in (A) mosquito (CxT), (B) human (A549), (C) avian (DF-1), (D) mammalian (Vero- 37°C), and (E) mammalian (Vero- 28°C) cell culture. Mean viral titers (log₁₀ pfu/ml) +/- SD are shown. Significant attenuation (paired t test, *p < 0.05, **p < 0.01, ***p < 0.001) was measured in all vertebrate cell lines side (B–E) but not in mosquito cell culture (A). Significantly greater differences in mean viral titers between WTic and NS3 P319L were measured in mammalian cell culture at 37°C relative to 28°C and in mammalian cell culture relative to avian (F; t test, *p < 0.05).

unexposed and NS3 P319L-exposed mosquitoes (Figure 4B; log rank test, p < 0.05). Additionally, mosquitoes infected with NS3 P319L that had disseminated infections (as indicated by positive legs) had increased mean longevity relative to mosquitoes with disseminated WTic infections (Figure 4C; log rank test, p < 0.01). These data suggest that NS3 P319L-exposed *Cx. pipiens* with the capacity for virus transmission have an increased probability of daily survival, which together with increased vector competence demonstrates a highly significant transmission advantage. No differences in the proportion of blood feeding or ovipositing were measured among groups.

In order to confirm the fitness advantage of NS3 P319L, a competition assay was completed in *Cx. pipiens*. WNV WTic and WNV NS3 P319L were mixed at a ratio of 1:4 (L319:P319), based on known stock titers, and used to create an infectious blood meal. Plaque morphology, which is highly distinct (Figure 1), was used to distinguish WT and mutant infectious particles. Blood meal titration confirmed an input of 7.0 log₁₀ pfu/ml WNV comprised of 27.0% WNV NS3 P319L (73.0% WTic). The infection rate of mosquitoes assayed at 14 days post-feeding, as determined by RT-PCR was 76.0% (19/25). Of these, 15 were found to have disseminated infections and 3 were found to have positive saliva. Body, leg, and saliva samples from the 3 mosquitoes with transmission capacity were plaque titrated in order to determine tissue-specific strain ratios and changes relative to input. An advantage was measured for WNV NS3 P319L in all output samples (Figure 5). Specifically, the mean percent of 319L in the three mosquito bodies tested at day 14 post-infection was 82.3%, which equates to a greater than 3-fold increase in WNV NS3 P319L relative to the blood meal proportion. This advantage further increased to 86.3% in corresponding legs, with no WNV WTic detected in 2/3 samples. Just one of the three RT-PCR-positive saliva samples had infectious virus above the limit of detection (100 pfu/mL), and no WNV WTic was detected in this sample. Together, this represents a highly significant increase in proportion of WNV NS3 P319L in all output samples relative to input proportions (Fisher's exact test, p < 0.0001), consistent with a significant fitness advantage in *Cx. pipiens* mosquitoes (Figure 5).

Decreased competence of WNV P319L in avian hosts

In order to determine if *in vitro* attenuation corresponded to decreased viral fitness in an avian host, 3-day-old chicks were inoculated subcutaneously with 100 pfu WNV WTic or WNV NS3 P319L and both viremia kinetics

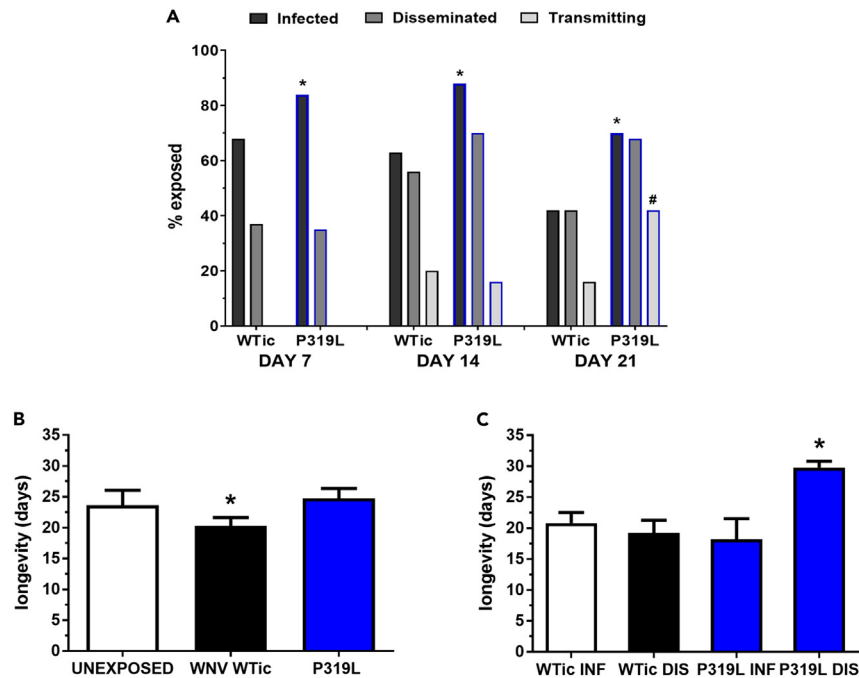


Figure 4. Increased transmissibility of West Nile virus NS3 P319L by *Cx. pipiens*

(A) Vector competence of *Cx. pipiens* for WNV WTic and WNV NS3 P319L. WNV positivity was determined in mosquito bodies (infection), legs (dissemination), and saliva (transmission) by qRT-PCR at days 7, 14, and 21 post-feeding on blood meals with $7.5 \log_{10}$ pfu/ml WNV. Increased infection rates for WNV NS3 P319L were measured at all time points (*chi-squared, $p < 0.01$), and increased transmission rates among exposed were measured at day 21 (#chi-squared, $p = 0.02$). (B and C) Mosquito longevity (shown as mean days survived \pm SEM) was monitored following blood feeding with WNV WTic, WNV NS3 P319L, or non-infectious blood (unexposed). Decreased survival was measured for WTic exposed mosquitoes relative to both unexposed and P319L-exposed mosquitoes (B, log rank test, * $p < 0.05$). This difference was primarily a result of a significant increase in mean survival of WNV P319L-exposed mosquitoes that developed disseminated infections (DIS) relative to infected mosquitoes without disseminated infections (INF) and WTic infected mosquitoes (C, log rank test, * $p < 0.05$).

and viral load in tissues were quantified. All chicks inoculated with WTic had detectable viremia at days 1–4 post-infection and WNV-positive brains and kidneys, while just 4/8 chicks inoculated with NS3 P319L developed detectable viremia and virus in tissues. Additionally, viremia was delayed in NS3 P319L-infected chicks for which there was detectable virus. Specifically, just one NS3 P319L-inoculated chick had detectable viremia on day 1 post-infection, with a quantified level of $2.2 \log_{10}$ pfu/ml. Conversely, all WTic-infected chicks had detectable viremia at day 1 post-infection, with a mean of $4.0 \log_{10}$ pfu/ml (Figure 6A). Mean viremia and tissue viral load (with negative specimens set to assay limit of detection [$0.7 \log_{10}$ pfu/ml]) were significantly lower for NS3 P319L (Figure 6; t tests, $p < 0.05$). To determine if selective pressure against 319L led to reversion, sequencing of output virus extracted from peak viremia serum samples was completed for the 4 viremic birds infected with WNV P319L. Analysis confirmed reversion to 319P in all samples.

Structure and function of NS3 319 are consistent with host-specific phenotypes

NS3 P319L is located in a highly conserved region across flaviviruses, a linker region between the N and C cores of the NS3 protein. Modeling of this mutation revealed that this linker region must undergo coordinated conformational changes for the N and the C core to move, a process which is critical for catalysis and, thus, unwinding of double-stranded RNA (dsRNA) (Figure 7). The substitution of a relatively flexible leucine in place of a structurally rigid proline could increase the flexibility of the linker region, leading to looser coordination of the N and C core movement, potentially having an effect on function.

Further probing of the effect of P319L on NS3 function via ATPase assay revealed highly significant phenotypic alterations resulting from this substitution. At 37°C , *in vitro* assessment of ATPase activity indicated negligible ADP production by NS3 P319L and significant attenuation relative to WT NS3 (Figure 8; linear regression

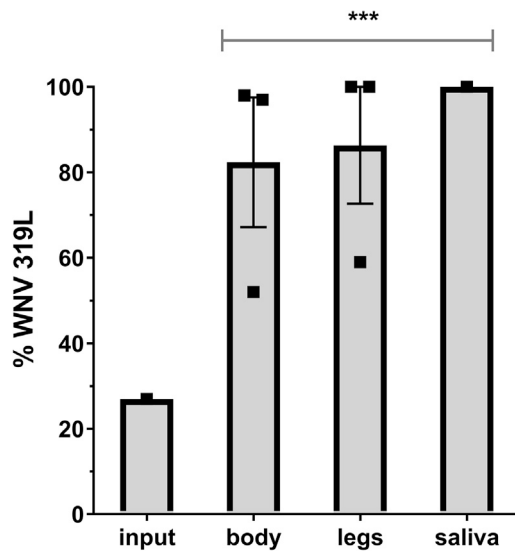


Figure 5. Increased fitness of West Nile virus NS3 P319L in *Cx. pipiens* following coinfection

Cx. pipiens mosquitoes were fed infectious blood meals with a ratio of 1:4 (L319:P319). Body, leg, and saliva samples were assayed on day 14 post-feeding and tested by RT-PCR. Ratios of virus strains (shown as mean % \pm SD) were determined by plaque size in the blood meal and tissues from the 3 mosquitoes determined to have positive saliva. A highly significant increase in proportion of WNV NS3 P319L in all output samples relative to input proportions was measured (**Fisher's exact test, $p < 0.0001$).

analysis, $p < 0.0001$). Given the temperature-dependent fitness identified both *in vivo* and, more directly, with *in vitro* growth assays (Figure 3), ATPase assays were additionally performed at 28°C. Strikingly, NS3 P319L demonstrated improved ATPase activity relative to WT NS3 at 28°C (Figure 8; linear regression analysis, $p = 0.002$).

DISCUSSION

While WNV and other arboviruses are known to be naturally maintained as quasispecies,¹⁵ and the relevance of intrahost diversity has been well-established using experimental systems,^{13,14,16,19,21,25–29} the phenotypic impact of naturally circulating minority variants on fitness and adaptation is largely unstudied. If the maintenance of diversity in nature to some extent facilitates host switching, then identifying minority genotypes with host-specific bias should provide insight into the mechanisms of host-specific fitness. Indeed, our results indicate that the WNV NS3 P319L substitution, a naturally occurring minority variant with a mosquito bias, confers host-specific fitness with attenuation in avian hosts and increased transmissibility by *Culex* mosquitoes.

In vitro results did not indicate an increase in replicative fitness in mosquito cells, yet experimental infections demonstrate that WNV NS3 P319L is both more infectious and less virulent than WT WNV in *Cx. pipiens*. While significant virulence in vectors is not regularly attributed to arboviruses, decreases in longevity and fecundity have been noted for numerous mosquito-borne viruses, including WNV in *Cx. pipiens*.³⁰ Importantly, the capacity to influence mosquito life-history traits has also been shown to be strain specific.³¹ We demonstrate that *Cx. pipiens* that develop disseminated WNV NS3 P319L infections have increased longevity relative to WNV WT-exposed mosquitoes, which together with increased infectivity would facilitate increased transmissibility and selection in mosquitoes. This transmission advantage was confirmed with a coinfection experiment demonstrating that a minority population of WNV P319L is likely to outcompete WT WNV in *Cx. pipiens*.

Initial *in vitro* studies revealed significant attenuation in mammalian cells in terms of cell-to-cell spread and replication, as well as a high level of reversion during multi-step growth. While mammals do not serve as amplifying hosts in WNV transmission and therefore do not exert selective pressure, WNV NS3 P319L was also modestly attenuated in avian cell culture. Experimental infection of chicks further demonstrated significant attenuation in terms of both viremia and viral load in tissues, as well as significant pressure for reversion. These results agree with the expected selective constraints on host-specific variants of arboviruses. If this mutation was neutral or advantageous to fitness in amplifying hosts, we would expect to find it fixed in consensus sequences, which is not the case.²² In fact, NS3 P319L was rarely identified in nature at intrahost levels greater than 10%, despite its significant advantage in mosquitoes. This is likely explained by the strong selective pressures against this mutation in birds. These results confirm that arboviruses can to some extent exploit minority diversity to overcome the adaptive constraints imposed by host cycling.

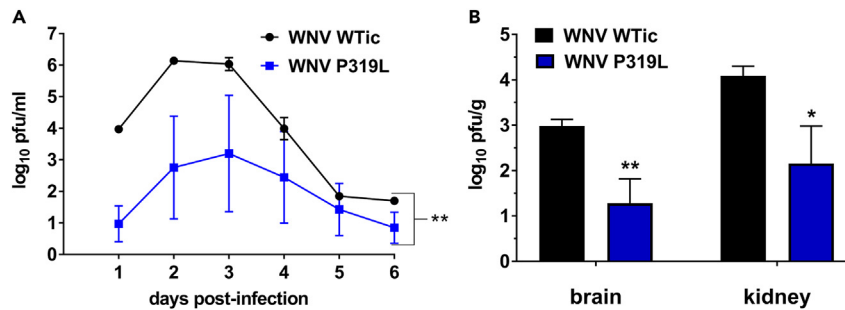


Figure 6. Attenuation of West Nile virus NS3 P319L in birds

Three-day-old chicks (*Gallus gallus*) were inoculated subcutaneously with 100 pfu WNV WTic or WNV NS3 P319L. (A and B) Viremia (A), evaluated at days 1–6 post-infection ($n = 4$ /timepoint, mean \pm SEM), was significantly lower for WNV P319L (**paired t test, $p = 0.01$). Viral load (B) in brain and kidney was evaluated at day 6 post-infection ($n = 8$, means \pm SEM) was significantly lower for WNV P319L in both tissues (t test, * $p = 0.04$, ** $p = 0.008$).

Although coinfection results demonstrate a competitive advantage for NS3 P319L in mosquitoes, we still investigated the phenotypic consequences in a relatively homogeneous population. In nature, intrahost populations consist of numerous coinfecting genotypes. Cooperative interactions with coinfecting strains,^{27,29} epistatic interactions with different genetic backgrounds,^{32,33} and the influence of diversity itself^{19,34} could all alter the phenotypic impact of this substitution in naturally diverse viral swarms. Further studies examining how NS3 P319L and other minority variants influence viral fitness in more realistic contexts could shed more light on the role of quasispecies structures in host-specific fitness.

Structural modeling revealed that NS3 P319 is a highly conserved residue across flaviviruses that is likely to influence catalysis.³⁵ Specifically, this residue is located in motif III of the linker region between the N and C cores of NS3, near the ATP hydrolysis active site. Residues in this motif have been shown to interact with other motifs and RecA-like domains to form the RNA binding cleft.³⁶ *In vitro* studies demonstrated that the attenuation of WNV NS3 P319L measured at 37°C in vertebrate cells was partially recovered at 28°C. Supporting this, ATPase activity of P319L is severely attenuated at 37°C but superior at 28°C, confirming temperature sensitivity consistent with phenotypic differences in birds and mosquitoes. The fact that replication is still supported to some extent at 37°C in avian cells without reversion suggests both that the lack of ATPase activity *in vitro* is not fully reflective of activity within the host cell and that NS3 P319L is not merely a temperature-sensitive substitution. Given the complexity of distinct host cell environments, it is perhaps unsurprising that an *in vitro* biochemical assay fails to fully recapitulate enzymatic activity *in vivo*. The replication complex itself may help to stabilize the NS3 to rescue ATPase function, and/or avian specific proteins may be influencing activity *in vivo*. Further evaluation of NS3 ATPase activity in complex with NS5 or other proteins in the replication complex, as well as probing NS3 interactions with host-specific proteins, could further clarify the mechanistic basis for cell-specific phenotypes.³⁷ Previous studies with WNV NS3 T249P suggest that increased virulence in birds is modulated by interactions with host proteins.²³ These studies also found temperature sensitivity at temperatures greater than 40°C, mimicking fever in birds.^{23,38} While we did not monitor body temperature in our study, virulence was not noted in any experimentally infected chick. It is possible that increased pressure for reversion and/or decreased virulence of WNV NS3 P319L would be noted in more competent host species such as corvids.

Perhaps most intriguing is the question of how increased ATPase activity could be associated with increased infectivity and decreased virulence in mosquitoes. Increased helicase unwinding could lead to increased replication efficiency, potentially facilitating the establishment of widespread midgut infection, yet we did not measure an obvious signature of increased replication for NS3 P319L in mosquitoes or mosquito cells. Although ATPase activity and helicase unwinding are often coupled, activity is not always correlative.^{23,39} Indeed, a previous study with Kunjin virus, considered a WNV subtype, demonstrated a higher rate of helicase activity without increased ATPase activity.⁴⁰ This study, in which residue S411 was mutated to alanine to disrupt a hydrogen bond that was hypothesized to stabilize secondary structure of the NS3 helicase, importantly demonstrated decreased infectivity, yet increased dissemination and virulence in *Cx quinquefasciatus*. It is possible that these phenotypes result from a downstream effect on other nonstructural proteins. Intriguingly, a recent study with DENV2 demonstrated that mutations in motif III of NS3 alter binding affinity to NS4B.⁴¹ While this is likely to perturb ATPase and/or helicase activity, it could

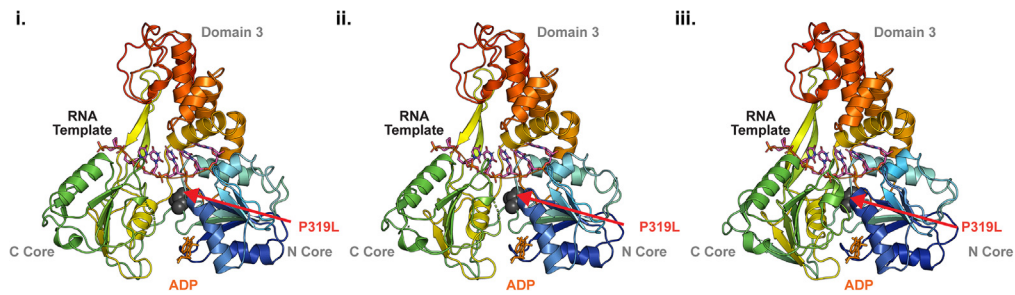


Figure 7. West Nile virus NS3 P319L is located in a conserved linker region responsible for coordinating catalysis
Panels i-iii show distinct conformations of the HCV helicase as it undergoes unwinding of the template RNA. Normally, this would result in translocation; however, the RNA template model was used from a single crystal structure (see [STAR Methods](#)) which renders it static in the other structures (2–3). The WNV helicase is well aligned with the represented HCV structure, indicating high similarity.

additionally alter the availability of this multifunctional protein to perform alternative functions, including its documented capacity to suppress RNA interference, the primary antiviral response in mosquitoes.^{42,43} Although the mechanism remains unclear, these results together suggest a role for the flavivirus NS3 in mosquito cell viability and permissiveness. Further studies exploiting host-specific variants could help facilitate a broader understanding of how arboviruses successfully navigate divergent host landscapes.

Limitations of the study

Although a naturally occurring minority mutation of WNV was studied in relevant hosts and vectors, there are important limitations to consider. First, while *Cx. pipiens* is a primary WNV vector globally, it is well-documented that transmissibility may be highly variable among distinct species and populations of mosquitoes, so the phenotypic consequences of this mutation could be distinct in other vector populations. Similarly, while chicks are a relevant model system, host competence, selective pressures, and viremia kinetics are variable among avian species. In addition, while competition assays demonstrate the relevance of this mutation during coinfection, natural infections comprise numerous haplotypes with increasing complexity and opportunities for both competition and cooperative interactions. Lastly, although the demonstration of temperature-dependent ATPase activity is in agreement with identified host-specific differences, there is the potential for additional biochemical consequences not assessed in this study.

STAR★METHODS

Detailed methods are provided in the online version of this paper and include the following:

- [KEY RESOURCES TABLE](#)
- [RESOURCE AVAILABILITY](#)
 - Lead contact
 - Data and code availability
- [MATERIALS AVAILABILITY](#)
- [EXPERIMENTAL MODEL AND STUDY PARTICIPANT DETAILS](#)
 - Mosquito cell culture
 - Vertebrate cell culture
 - *Culex pipiens*
 - *Gallus gallus*
- [METHOD DETAILS](#)
 - Reverse genetics
 - Virus quantification
 - Viral growth kinetics
 - Structural modeling
 - Vector competence
 - Mosquito life-history traits
 - Avian competence

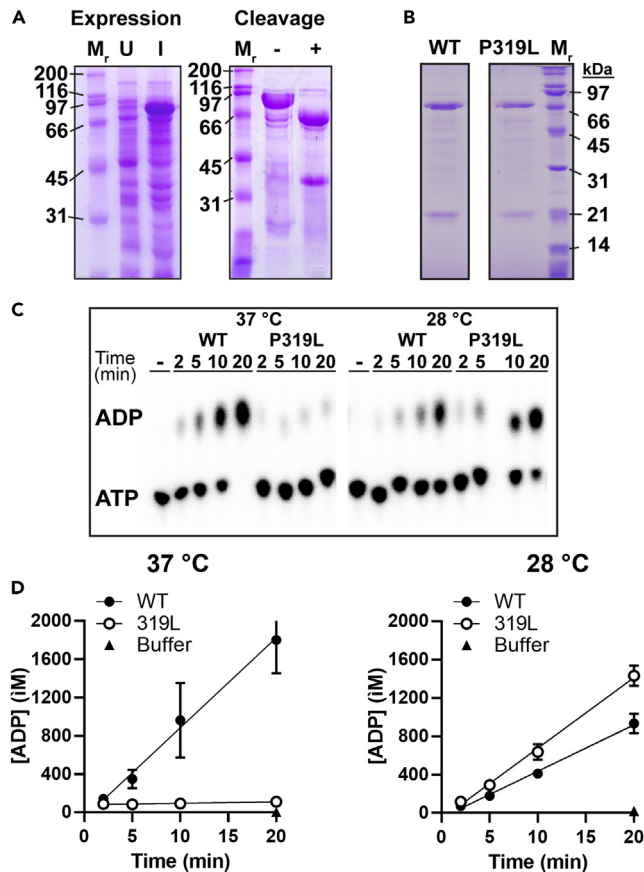


Figure 8. West Nile virus NS3 P319L demonstrates temperature-sensitive ATPase activity

(A) Purification scheme of WNV NS3. We expressed and purified NS3 as described in the STAR Methods. Progress was visualized by electrophoresis through a 10% polyacrylamide gel. Cells were induced (U: uninduced, I: induced), lysed, centrifuged, and eluted from an Ni-NTA column. Protein was treated with the Ulp1 protease (before: -, after: +) to remove the N-terminal SUMO protein.

(B) Purified proteins used in this study. Molecular weight standards (M_r) in panels A and B are represented in kDa.

(C) Primary data of NS3-mediated ATPase assay. A phosphorimage of a PEI-TLC plate shows a time course of hydrolysis of ATP (2 mM) to ADP in the presence of 300 nM NS3 protein. Buffer was used as a negative control (-). Further reaction details are available in the Materials and Methods.

(D) ATPase activity of WTic NS3 and P319L NS3 were compared. A significantly higher rate of ADP formation was measured at 28°C for P319L (A; linear regression analysis, $p = 0.02$) and significantly lower rate of ADP formation was measured at 37°C for P319L (B; linear regression analysis, $p < 0.0001$) Error bars represent SD, $n = 3-4$.

- Construction of WNV NS3 bacterial expression plasmids
- Expression and purification of WNV NS3
- NS3 ATPase activity and quantification
- **QUANTIFICATION AND STATISTICAL ANALYSIS**

SUPPLEMENTAL INFORMATION

Supplemental information can be found online at <https://doi.org/10.1016/j.isci.2023.107468>.

ACKNOWLEDGMENTS

We thank the Wadsworth Center Advanced Genomic Technologies Core for sequencing, the Wadsworth Center Tissue and Media Facility for providing media and cells, and the NYS Arbovirus Laboratory insectary staff for support and assistance. These studies were funded by the National Institutes of Health (R21 AI146856 (ATC), R01 AI168097 (ATC), and R01 AI169462 (CEC)).

AUTHOR CONTRIBUTIONS

Conceptualization, A.T.C., H.S.C.; Methodology, A.T.C, H.S.C., L.K., J.D.P, A.P.D., J.J.A., C.E.C.; Investigation, H.S.C., L.K., J.D.P, A.P.D., J.J.A., C.Y., A.F.P., J.S., C.A.K., S.M.B., E.M.B., T.A.N.; Writing – Original Draft, A.T.C., H.S.C.; Writing – Review & Editing, A.T.C., H.S.C, A.P.D., J.J.A., C.Y., E.M.B., C.E.C.; Funding Acquisition, A.T.C., C.E.C, J.J.A.; Resources, A.T.C., C.E.C.; Supervision, A.T.C., J.D.P, J.J.A., C.E.C.

DECLARATION OF INTERESTS

The authors declare no competing interests.

Received: September 27, 2022

Revised: June 22, 2023

Accepted: July 21, 2023

Published: July 26, 2023

REFERENCES

- Ronca, S.E., Ruff, J.C., and Murray, K.O. (2021). A 20-year historical review of West Nile virus since its initial emergence in North America: Has West Nile virus become a neglected tropical disease? *PLoS Negl. Trop. Dis.* 15, e0009190. <https://doi.org/10.1371/journal.pntd.0009190>.
- Chancey, C., Grinev, A., Volkova, E., and Rios, M. (2015). The global ecology and epidemiology of West Nile virus. *BioMed Res. Int.* 2015, 376230. <https://doi.org/10.1155/2015/376230>.
- Kramer, L.D., Styer, L.M., and Ebel, G.D. (2008). A global perspective on the epidemiology of West Nile virus. *Annu. Rev. Entomol.* 53, 61–81. [doi]. <https://doi.org/10.1146/annurev.ento.53.103106.093258>.
- Colpitts, T.M., Conway, M.J., Montgomery, R.R., and Fikrig, E. (2012). West Nile Virus: biology, transmission, and human infection. *Clin. Microbiol. Rev.* 25, 635–648. 25/4/635 [pii]. <https://doi.org/10.1128/CMR.00045-12>.
- Hayes, E.B., Komar, N., Nasci, R.S., Montgomery, S.P., O’Leary, D.R., and Campbell, G.L. (2005). Epidemiology and transmission dynamics of West Nile virus disease. *Emerg. Infect. Dis.* 11, 1167–1173.
- Lauring, A.S., and Andino, R. (2010). Quasispecies theory and the behavior of RNA viruses. *PLoS Pathog.* 6, e1001005.
- Steinhauer, D.A., Domingo, E., and Holland, J.J. (1992). Lack of evidence for proofreading mechanisms associated with an RNA virus polymerase. *Gene* 122, 281–288. [https://doi.org/10.1016/0378-1119\(92\)90216-c](https://doi.org/10.1016/0378-1119(92)90216-c).
- Drake, J.W., and Holland, J.J. (1999). Mutation rates among RNA viruses. *Proc. Natl. Acad. Sci. USA.* 96, 13910–13913.
- Caldwell, H.S., Lasek-Nesselquist, E., Follano, P., Kramer, L.D., and Ciota, A.T. (2020). Divergent Mutational Landscapes of Consensus and Minority Genotypes of West Nile Virus Demonstrate Host and Gene-Specific Evolutionary Pressures. *Genes* 11, 1299. <https://doi.org/10.3390/genes11111299>.
- Parameswaran, P., Wang, C., Trivedi, S.B., Eswarappa, M., Montoya, M., Balmaseda, A., and Harris, E. (2017). Intrahost Selection Pressures Drive Rapid Dengue Virus Microevolution in Acute Human Infections. *Cell Host Microbe* 22, 400–410.e5. <https://doi.org/10.1016/j.chom.2017.08.003>.
- Vignuzzi, M., Stone, J.K., Arnold, J.J., Cameron, C.E., and Andino, R. (2006). Quasispecies diversity determines pathogenesis through cooperative interactions in a viral population. *Nature* 439, 344–348. <https://doi.org/10.1038/nature04388>.
- Dridi, M., Rosseel, T., Orton, R., Johnson, P., Lecollinet, S., Muylkens, B., Lambrecht, B., and Van Borm, S. (2015). Next-generation sequencing shows West Nile virus quasispecies diversification after a single passage in a carrion crow (*Corvus corone*) *in vivo* infection model. *J. Gen. Virol.* 96, 2999–3009. <https://doi.org/10.1099/jgv.0.000231>.
- Jerzak, G.V.S., Brown, I., Shi, P.-Y., Kramer, L.D., and Ebel, G.D. (2008). Genetic diversity and purifying selection in West Nile virus populations are maintained during host switching. *Virology* 374, 256–260. <https://doi.org/10.1016/j.virol.2008.02.032>.
- Jerzak, G.V.S., Bernard, K., Kramer, L.D., Shi, P.Y., and Ebel, G.D. (2007). The West Nile virus mutant spectrum is host-dependant and a determinant of mortality in mice. *Virology* 360, 469–476.
- Jerzak, G., Bernard, K.A., Kramer, L.D., and Ebel, G.D. (2005). Genetic variation in West Nile virus from naturally infected mosquitoes and birds suggests quasispecies structure and strong purifying selection. *J. Gen. Virol.* 86, 2175–2183.
- Ciota, A.T., Ngo, K.A., Lovelace, A.O., Payne, A.F., Zhou, Y., Shi, P.-Y., and Kramer, L.D. (2007). Role of the mutant spectrum in adaptation and replication of West Nile virus. *J. Gen. Virol.* 88, 865–874.
- Ciota, A.T., Jia, Y., Payne, A.F., Jerzak, G., Davis, L.J., Young, D.S., Ehrbar, D., and Kramer, L.D. (2009). Experimental passage of St. Louis encephalitis virus *in vivo* in mosquitoes and chickens reveals evolutionarily significant virus characteristics. *PLoS One* 4, e7876.
- Coffey, L.L., Beeharry, Y., Bordería, A.V., Blanc, H., and Vignuzzi, M. (2011). Arbovirus high fidelity variant loses fitness in mosquitoes and mice. *Proc. Natl. Acad. Sci. USA.* 108, 16038–16043. 1111650108 [pii]. <https://doi.org/10.1073/pnas.1111650108>.
- Van Slyke, G.A., Arnold, J.J., Lugo, A.J., Griesemer, S.B., Moustafa, I.M., Kramer, L.D., Cameron, C.E., and Ciota, A.T. (2015). Sequence-Specific Fidelity Alterations Associated with West Nile Virus Attenuation in Mosquitoes. *PLoS Pathog.* 11, e1005009. <https://doi.org/10.1371/journal.ppat.1005009>.
- Griesemer, S.B., Kramer, L.D., Van Slyke, G.A., Pata, J.D., Gohara, D.W., Cameron, C.E., and Ciota, A.T. (2017). Mutagen resistance and mutation restriction of St. Louis encephalitis virus. *J. Gen. Virol.* 98, 201–211. <https://doi.org/10.1099/jgv.0.000682>.
- Caldwell, H.S., Ngo, K., Pata, J.D., Kramer, L.D., and Ciota, A.T. (2020). West Nile Virus fidelity modulates the capacity for host cycling and adaptation. *J. Gen. Virol.* 101, 410–419. <https://doi.org/10.1099/jgv.0.001393>.
- Bialosuknia, S.M., Tan, Y., Zink, S.D., Koetner, C.A., Maffei, J.G., Halpin, R.A., Muller, E., Novatny, M., Shilts, M., Fedorova, N.B., et al. (2019). Evolutionary dynamics and molecular epidemiology of West Nile virus in New York State: 1999–2015. *Virus evolution* 5, vez020. <https://doi.org/10.1093/ve/vez020>.
- Langevin, S.A., Bowen, R.A., Reisen, W.K., Andrade, C.C., Ramey, W.N., Maharaj, P.D., Anishchenko, M., Kenney, J.L., Duggal, N.K., Romo, H., et al. (2014). Host competence and helicase activity differences exhibited by West Nile viral variants expressing NS3-249 amino acid polymorphisms. *PLoS One* 9, e100802. <https://doi.org/10.1371/journal.pone.0100802>.
- Caldwell, H.S., Pata, J.D., and Ciota, A.T. (2022). The Role of the Flavivirus Replicase in

- Viral Diversity and Adaptation. *Viruses* 14, 1076. <https://doi.org/10.3390/v14051076>.
25. Fitzpatrick, K.A., Deardorff, E.R., Pesko, K., Brackney, D.E., Zhang, B., Bedrick, E., Shi, P.Y., and Ebel, G.D. (2010). Population variation of West Nile virus confers a host-specific fitness benefit in mosquitoes. *Virology* 404, 89–95.
 26. Grubaugh, N.D., Smith, D.R., Brackney, D.E., Bosco-Lauth, A.M., Fauver, J.R., Campbell, C.L., Felix, T.A., Romo, H., Duggal, N.K., Dietrich, E.A., et al. (2015). Experimental evolution of an RNA virus in wild birds: evidence for host-dependent impacts on population structure and competitive fitness. *PLoS Pathog.* 11, e1004874. <https://doi.org/10.1371/journal.ppat.1004874>.
 27. Ebel, G.D., Fitzpatrick, K.A., Lim, P.Y., Bennett, C.J., Deardorff, E.R., Jerzak, G.V.S., Kramer, L.D., Zhou, Y., Shi, P.Y., and Bernard, K.A. (2011). Nonconsensus West Nile virus genomes arising during mosquito infection suppress pathogenesis and modulate virus fitness *in vivo*. *J. Virol.* 85, 12605–12613. *JVI.* 05637-11 [pii]. <https://doi.org/10.1128/JVI.05637-11>.
 28. Ciota, A.T., Ehrbar, D.J., Van Slyke, G.A., Payne, A.F., Willsey, G.G., Viscio, R.E., and Kramer, L.D. (2012). Quantification of intrahost bottlenecks of West Nile virus in *Culex pipiens* mosquitoes using an artificial mutant swarm. *Infect. Genet. Evol.* 12, 557–564. S1567-1348(12)00023-8 [pii]. <https://doi.org/10.1016/j.meegid.2012.01.022>.
 29. Ciota, A.T., Ehrbar, D.J., Van Slyke, G.A., Willsey, G.G., and Kramer, L.D. (2012). Cooperative interactions in the West Nile virus mutant swarm. *BMC Evol. Biol.* 12, 58. 1471-2148-12-58 [pii]. <https://doi.org/10.1186/1471-2148-12-58>.
 30. Ciota, A.T., Styer, L.M., Meola, M.A., and Kramer, L.D. (2011). The costs of infection and resistance as determinants of West Nile virus susceptibility in *Culex* mosquitoes. *BMC Ecol.* 11, 23. 1472-6785-11-23 [pii]. <https://doi.org/10.1186/1472-6785-11-23>.
 31. Ciota, A.T., Ehrbar, D.J., Matarachio, A.C., Van Slyke, G.A., and Kramer, L.D. (2013). The evolution of virulence of West Nile virus in a mosquito vector: implications for arbovirus adaptation and evolution. *BMC Evol. Biol.* 13, 71–1471. 2148-13-71 [pii]. <https://doi.org/10.1186/1471-2148-13-71>.
 32. Chu, P.Y., Ke, G.M., Chen, P.C., Liu, L.T., Tsai, Y.C., and Tsai, J.J. (2013). Spatiotemporal dynamics and epistatic interaction sites in dengue virus type 1: a comprehensive sequence-based analysis. *PLoS One* 8, e74165. <https://doi.org/10.1371/journal.pone.0074165>.
 33. Agarwal, A., Sharma, A.K., Sukumaran, D., Parida, M., and Dash, P.K. (2016). Two novel epistatic mutations (E1:K211E and E2:V264A) in structural proteins of Chikungunya virus enhance fitness in *Aedes aegypti*. *Virology* 497, 59–68. <https://doi.org/10.1016/j.virol.2016.06.025>.
 34. Brackney, D.E., Beane, J.E., and Ebel, G.D. (2009). RNAi targeting of West Nile virus in mosquito midguts promotes virus diversification. *PLoS Pathog.* 5, e1000502.
 35. Maruyama, S.R., Castro-Jorge, L.A., Ribeiro, J.M.C., Gardinassi, L.G., Garcia, G.R., Brandão, L.G., Rodrigues, A.R., Okada, M.I., Abrão, E.P., Ferreira, B.R., et al. (2014). Characterisation of divergent flavivirus NS3 and NS5 protein sequences detected in *Rhipicephalus microplus* ticks from Brazil. *Mem. Inst. Oswaldo Cruz* 109, 38–50. <https://doi.org/10.1590/0074-0276130166>.
 36. Du Pont, K.E., McCullagh, M., and Geiss, B.J. (2022). Conserved motifs in the flavivirus NS3 RNA helicase enzyme. *Wiley Interdiscip. Rev. RNA* 13, e1688. <https://doi.org/10.1002/wrna.1688>.
 37. Wu, J., Bera, A.K., Kuhn, R.J., and Smith, J.L. (2005). Structure of the Flavivirus helicase: implications for catalytic activity, protein interactions, and proteolytic processing. *J. Virol.* 79, 10268–10277. <https://doi.org/10.1128/JVI.79.16.10268-10277.2005>.
 38. Kinney, R.M., Huang, C.Y.H., Whiteman, M.C., Bowen, R.A., Langevin, S.A., Miller, B.R., and Brault, A.C. (2006). Avian virulence and thermostable replication of the North American strain of West Nile virus. *J. Gen. Virol.* 87, 3611–3622. <https://doi.org/10.1099/vir.0.82299-0>.
 39. Du Pont, K.E., Davidson, R.B., McCullagh, M., and Geiss, B.J. (2020). Motif V regulates energy transduction between the flavivirus NS3 ATPase and RNA-binding cleft. *J. Biol. Chem.* 295, 1551–1564. <https://doi.org/10.1074/jbc.RA119.011922>.
 40. Du Pont, K.E., Sexton, N.R., McCullagh, M., Ebel, G.D., and Geiss, B.J. (2020). A Hyperactive Kunjin Virus NS3 Helicase Mutant Demonstrates Increased Dissemination and Mortality in Mosquitoes. *J. Virol.* 94, e01021-20. <https://doi.org/10.1128/JVI.01021-20>.
 41. Lu, H., Zhan, Y., Li, X., Bai, X., Yuan, F., Ma, L., Wang, X., Xie, M., Wu, W., and Chen, Z. (2021). Novel insights into the function of an N-terminal region of DENV2 NS4B for the optimal helicase activity of NS3. *Virus Res.* 295, 198318. <https://doi.org/10.1016/j.virusres.2021.198318>.
 42. Kakumani, P.K., Ponia, S.S., S, R.K., Sood, V., Chinnappan, M., Banerjee, A.C., Medigeshi, G.R., Malhotra, P., Mukherjee, S.K., and Bhatnagar, R.K. (2013). Role of RNA interference (RNAi) in dengue virus replication and identification of NS4B as an RNAi suppressor. *J. Virol.* 87, 8870–8883. <https://doi.org/10.1128/JVI.02774-12>.
 43. Zmurko, J., Neyts, J., and Dallmeier, K. (2015). Flaviviral NS4b, chameleon and jack-in-the-box roles in viral replication and pathogenesis, and a molecular target for antiviral intervention. *Rev. Med. Virol.* 25, 205–223. <https://doi.org/10.1002/rmv.1835>.
 44. Bialosuknia, S.M., Dupuis II, A.P., Zink, S.D., Koetzner, C.A., Maffei, J.G., Owen, J.C., Landwerlen, H., Kramer, L.D., and Ciota, A.T. (2022). Adaptive evolution of West Nile virus facilitated increased transmissibility and prevalence in New York State. *Emerg. Microbes Infect.* 11, 988–999. <https://doi.org/10.1080/22221751.2022.2056521>.
 45. Fay, R.L., Ngo, K.A., Kuo, L., Willsey, G.G., Kramer, L.D., and Ciota, A.T. (2021). Experimental Evolution of West Nile Virus at Higher Temperatures Facilitates Broad Adaptation and Increased Genetic Diversity. *Viruses* 13, 1889.
 46. Payne, A.F., Binduga-Gajewska, I., Kauffman, E.B., and Kramer, L.D. (2006). Quantitation of flaviviruses by fluorescent focus assay. *J. Virol. Methods* 134, 183–189.
 47. Lanciotti, R.S., Kerst, A.J., Nasci, R.S., Godsey, M.S., Mitchell, C.J., Savage, H.M., Komar, N., Panella, N.A., Allen, B.C., Volpe, K.E., et al. (2000). Rapid detection of West Nile virus from human clinical specimens, field-collected mosquitoes, and avian samples by a TaqMan reverse transcriptase-PCR assay. *J. Clin. Microbiol.* 38, 4066–4071.
 48. Schrodinger, L.L.C. (2015). The PyMOL Molecular Graphics System. Version 1.8.
 49. Mastrangelo, E., Milani, M., Bollati, M., Selisko, B., Peyrane, F., Pandini, V., Sorrentino, G., Canard, B., Konarev, P.V., Svergun, D.I., et al. (2007). Crystal structure and activity of Kunjin virus NS3 helicase; protease and helicase domain assembly in the full length NS3 protein. *J. Mol. Biol.* 372, 444–455. S0022-2836(07)00844-3 [pii]. <https://doi.org/10.1016/j.jmb.2007.06.055>.
 50. Kim, J.L., Morgenstern, K.A., Griffith, J.P., Dwyer, M.D., Thomson, J.A., Murcko, M.A., Lin, C., and Caron, P.R. (1998). Hepatitis C virus NS3 RNA helicase domain with a bound oligonucleotide: the crystal structure provides insights into the mode of unwinding. *Structure* 6, 89–100. [https://doi.org/10.1016/s0969-2126\(98\)00010-0](https://doi.org/10.1016/s0969-2126(98)00010-0).
 51. Gu, M., and Rice, C.M. (2016). The Spring alpha-Helix Coordinates Multiple Modes of HCV (Hepatitis C Virus) NS3 Helicase Action. *J. Biol. Chem.* 291, 14499–14509. <https://doi.org/10.1074/jbc.M115.704379>.
 52. Arnold, J.J., Bernal, A., Uche, U., Sterner, D.E., Butt, T.R., Cameron, C.E., and Mattern, M.R. (2006). Small ubiquitin-like modifying protein isopeptidase assay based on poliovirus RNA polymerase activity. *Anal. Biochem.* 350, 214–221. S0003-2697(05)00796-7 [pii]. <https://doi.org/10.1016/j.ab.2005.11.001>.
 53. Studier, F.W. (2005). Protein production by auto-induction in high density shaking cultures. *Protein Expr. Purif.* 41, 207–234. <https://doi.org/10.1016/j.pep.2005.01.016>.

STAR★METHODS

KEY RESOURCES TABLE

REAGENT or RESOURCE	SOURCE	IDENTIFIER
Antibodies		
Goat anti-mouse IgG FITC	Invitrogen	Cat # F-2761
pan flaviviral anti-E protein monoclonal antibody clone 4G2	Dr. Hongmin Li	C4G2A
Bacterial and virus strains		
<i>E. coli</i> Rosetta (DE3)	Dr. Craig E Cameron Lab	DE3
<i>E. coli</i> DH5 α	Dr. Craig E Cameron Lab	DH5 α
<i>E. coli</i> 10-beta	New England Biolabs	Cat. #C3019H
WNV NS3 P319L mutant virus	This paper	WNV NS3 P319L
WNV WTic (WNV02 WT)	This paper	WNV WTic
Chemicals, peptides, and recombinant proteins		
2-mercaptoethanol	MP Biomedicals	Cat# 190242
Pepstatin A	Alfa Aesar	Cat# J60237-25MG
Leupeptin	Amresco	Cat# J580-25MG
Kanamycin sulfate	VWR	Cat# 0408-25G
Chloramphenicol	Amresco	Cat# 0230-100G
Imidazole	Alfa Aesar	Cat# A10221
Ammonium Sulfate	Sigma Aldrich	Cat# A4418
Polyethylenimine (PEI)	Sigma Aldrich	Cat# P3143
Tris(2-carboxyethyl)phosphine hydrochloride solution (TCEP)	Sigma Aldrich	Cat# 646547-10X1ML
Phenylmethylsulfonylfluoride (PMSF)	Thermo Scientific	Cat# 36978
NP-40	Thermo Scientific	Cat# 85124
Critical commercial assays		
Q5 High Fidelity	New England Biolabs	Cat# M0491S
NEBuilder HiFi DNA Assembly	New England Biolabs	Cat #E5520S
Zymo DNA Clean and Concentrator	Zymo Research	Cat# D4004
JetMESSENGER mRNA transfection reagent	Polyplus	Cat# 101000005
HiScribe® T7 ARCA mRNA Kit	New England Biolabs	Cat# E2065S
Experimental models: Cell lines		
<i>Culex tarsalis</i> mosquitoes	Aaron Brault, CDC	CT
African green monkey (Vero)	ATCC	CCL-81
Chicken embryo fibroblast	ATCC	CRL-141
Human lung epithelial	ATCC	CCL-185
Experimental models: Organisms/strains		
<i>Culex pipiens</i> mosquitoes	NYS Arbovirus Lab	PA
<i>Gallus gallus</i> (1-day old specific-pathogen free chicks)	Charles River Labs	Cat# 10100336
Oligonucleotides		
Primer pairs for WNV sequencing: pair 1: AGTAGTTCGCCTGTGTGAGCTGAC, GAGAGCCCCAGCAATCC, pair 2: CCTTGCAAAGTTCCTATCTC, CTCTGCC AGCCCTCCGACGAT, pair 3: GGACCAACCAGGAGAACATT, GATCCGAGT ACACCTGGCGTCAA, pair 4: CAAGGCGAGCAGGGTGTAT, GAAGCTCGAC TCACCCAATACAT, pair 5: GCTCTGCCCTACATGCCGAAAGT, CGGCTGA GTCTTTCTTCCCATTC, pair 6: TGAGGAGCGCGAGGCACAT, AGATCCTG TGTTCTCGCACCACCAGC	Bialosuknia et al. ⁴⁴ Integrated DNA Technologies	WNV seq r/f 1-6

(Continued on next page)

Continued

REAGENT or RESOURCE	SOURCE	IDENTIFIER
P319L NS3 forward primer mutagenesis ATGACAGCCACCCTACCCGGGACTTCA GATCCATTCCCAGAGTCCAATTC	Integrated DNA Technologies	WNV 319Lf
P319L NS3 reverse primer TGGATCTGAAG TCCCGGTAGGGTGGCTGTCATGAATA TTGCCGC	Integrated DNA Technologies	WNV 319Lr
Recombinant DNA		
pSUMO-WNV-NS3 plasmid	Dr. Craig E Cameron	pSUMO-WNV-NS3
Software and algorithms		
ImageQuant TL software	Cytiva	ImageQuant TL800
rowheadOther		
Ubiquitin-like-specific protease (Ulp1)	Dr. Craig E Cameron	Ulp1
Ni-NTA Agarose	Qiagen	Cat# 30210
Polyethyleneimine-cellulose TLC plates	Millipore Sigma	Cat# M1055790001
$\alpha^{32}\text{P}$ -ATP	Perkin Elmer	Cat# BLU003H250UC
Dialysis tubing	Spectrum Spectra/Por	Cat# 86966

RESOURCE AVAILABILITY**Lead contact**

Further information and requests for resources should be directed to and will be fulfilled by the lead contact, Alexander Ciota (alexander.ciota@health.ny.gov).

Data and code availability**Data**

All data reported in this paper will be shared by the [lead contact](#) upon request.

Code

This paper does not report original code.

Any additional information required to reanalyze the data reported in this paper is available from the [lead contact](#) upon request.

MATERIALS AVAILABILITY

This study did not generate new unique reagents.

EXPERIMENTAL MODEL AND STUDY PARTICIPANT DETAILS**Mosquito cell culture**

Culex tarsalis cells (CxT) were originally provided by A. Brault (CDC, Ft Collins, CO) and maintained at the Wadsworth Center Tissue and Media Facility. CxT cells were grown at an optimum temperature of 28°C with 5.0% CO₂. Schneider's media with 10% Fetal Bovine Serum was used for growth and maintenance. Maintenance and infection were completed using six-well plates (Corning Costar, Cambridge, MA, USA) with 5 × 10⁶ cells/well. Three mL of media was used for maintenance.

Vertebrate cell culture

Vero (African green monkey kidney), DF-1 (Chicken embryo fibroblast) and A549 (Human lung epithelial carcinoma) were originally obtained from ATCC (CCL-81, CRL-141, CCL-185, respectively) and maintained at the Wadsworth Center Tissue and Media Facility. Eagle's minimum essential media with 10% Fetal Bovine Serum was used for growth and maintenance and all cells were maintained at 37°C with 5% CO₂.

Maintenance and infection were completed using six-well plates (Corning Costar, Cambridge, MA, USA) with 1×10^6 cells/well. Three mL of media was used for maintenance.

Culex pipiens

Cx. pipiens egg rafts were originally collected in Pennsylvania in 2004 (courtesy of Michael Hutchinson, Pennsylvania State University, PA, USA) and colonized at the Arbovirus Laboratories, Wadsworth Center, NYS Dept of Health. Mosquitoes were reared and maintained in 12" x 12" x 12" cages in an environmental chamber at 27°C, 50-65% relative humidity, with a photoperiod of 16: 8 h (light: dark). Immature stages are maintained in flats with 1L distilled water, 200 larvae/flat, and fed a 1:1 mixture of Koi food and Rabbit pellets. Adult female mosquitoes are offered blood meals with chicken blood and 2.5% sucrose once a week. Mosquitoes used for experiments were kept in mesh-top 1 quart paper cartons and provided with cotton pads soaked in 10% sucrose *ad libitum*. Mosquitoes were kept for 4–7 days before being transferred to cups for experimental infections in the BSL-3 facility.

Gallus gallus

Day-old, specific-pathogen-free chickens (*Gallus gallus*) were obtained from Charles River Laboratories (New York, NY). Sex determination of chicks is not completed as it is unreliable and not known to effect experimental outcomes. Upon arrival chicks are placed in brooder cages (8 chicks/cage for the three WNV-infected groups, 4 chicks/cage for uninfected group). Chicks are housed in wire cages (approximately 36" x 24" x 10") according to size of birds with a removable pad changed as needed every 1-2 days. A ceramic heat lamp or an infrared lamp is placed adjacent to the cages to provide warmth. The chicks are provided with food (chick starter) and water *ad libitum*. High and low room temperatures are measured with digital readers placed within rooms that read out min/max temperature values over previous 24-hour period. A laser thermometer is used to record the temperature within the brooder box to ensure all chicks have access to temperatures of at least 95°F. Infected animals are observed at least twice daily. All procedures for experimental infection of chicks were approved by the Wadsworth Center IACUC, New York State Department of Health (21-355).

METHOD DETAILS

Reverse genetics

Mutagenesis of an established WNV infectious clone (WTic) was completed to create WNV NS3P319L.⁴⁵ The construct utilizes a system of two plasmids, pWNV02-5'half and pWNV02-3'half, each containing half of the WNV cDNA cloned into the low copy-number vector pACYC177. The first plasmid contains the 5' half of the WNV02 genome preceded by the T7 RNA polymerase promoter and bounded at its 3' end by the unique BsiWI site in NS3. The second plasmid contains the 3' half of the WNV02 genome, running from the BsiWI site through the 3' UTR, followed by an engineered XbaI site which upon digestion will yield the 3'terminus of WNV cDNA template. The NS3 mutation was introduced into pWNV02-5'half by PCR mutagenesis. Full-length templates for mutants were created by *in vitro* ligation of BsiWI-cut pWNV02-5'half to the BsiWI-XbaI fragment excised from pWNV02-3'half. Capped, full-length RNA genomes were synthesized *in vitro* using HiScribe T7 ARCA mRNA kit (New England Biosystems) per the manufacturer's instructions, prior to electroporation into *Aedes albopictus* (C6/36) cells. Viral supernatant from transfected C6/36 cells was harvested after signs of cytopathic effect (CPE) and subsequently amplified once in C6/36 cells, where it was harvested and acted as the final stock used. The viral genome of this stock was confirmed via whole genome sequencing of 6 RT-PCR fragments on the Illumina MiSeq platform.⁹

Virus quantification

Plaque titration was performed in order to quantify WNV.⁴⁶ Six-well confluent monolayers of Vero cells were infected with 100 microliters of 10-fold dilutions of viral stock for one hour at 37°C. Plates were then overlaid with 3 ml warm 1:1 mixture of 2x EMEM with 10% fetal bovine serum (FBS) media and oxid agar. Plates were incubated at 37°C for two days, at which point they were overlaid with a 1:1 mixture of 2x EMEM 2% FBS and agar with the addition of neutral red to a final concentration of 1.5%. Plaques were counted 24 h after staining.

Quantitative reverse transcriptase polymerase chain reaction (qRT-PCR) was performed as in.⁴⁵ RNA was extracted using the manufacturer's protocol in the MagMAX apparatus (Applied Biosystems) using a Tecan Evo 150 liquid handler (Tecan). Real-time quantitative RT-PCR was completed on the Quant Studio 5 or

using the Applied Biosystems 7500 Fast Real Time PCR instrument using TaqMan One-Step RT-PCR. Primers against the envelope protein were utilized with the probe⁴⁷ and copy-number standards were used for quantification.

Fluorescent focus assays (FFA) were performed as in⁴⁶ to determine viral spread in distinct host cell types, including Vero and DF-1. Cells were seeded at a concentration such that confluency was achieved after two days of growth in an 8-well slide chamber. Cells were then infected with candidate virus at 3 different concentrations, depending on cell type. For Vero and DF-1 cells, concentrations ranged from 2×10^6 pfu/ml to 2×10^4 pfu/ml. Fifty microliters of inoculum was used to infect wells, which were placed at cell appropriate temperatures for one hour. Wells were then overlaid with semi-solid overlay of 2x growth media with 1.6% carboxymethyl cellulose (CMC). Following 24 (Vero) or 48 hours (DF-1), overlay was removed, and cells were washed with phosphate buffered saline (PBS) containing 0.2% bovine serum albumin (BSA). Cells were fixed with cold methanol on ice for 10 minutes. Methanol was removed and cells rinsed prior to the addition of 25 μ l primary antibody (murine pan flaviviral anti-E protein; received from Dr. Hongmin Li), diluted 1:150 in PBS-BSA solution. Cells were incubated at room temperature in moist chamber, for one hour, then washed three times in PBS-BSA. Secondary antibody (Goat anti-mouse IgG FITC, Invitrogen) diluted 1:150 as before was added and incubated for 30 minutes. Cells were washed three times as before and mounting media (25% glycerol and tris-HCL) added. Coverslips were affixed with white clear nail polish. Results were visualized using a Keyence BZ-X810 to detect FITC fluorescence. Foci area was measured and averaged for each virus and cell type.

Viral growth kinetics

Growth kinetics were performed as in.²¹ Cells were allowed to become confluent on six-well plates in cell appropriate media: EMEM 10% FBS for African Green Monkey Kidney cells (Vero) and adenocarcinoma human alveolar epithelial cells (A549), Dulbecco's modified essential media (DMEM) with 10% FBS for chicken fibroblast cells (DF-1), or Schneider's media 10% FBS for *Culex tarsalis* cells (CxT). Maintenance media used for a liquid overlay after infection for each cell line were identical except 10% FBS was replaced by 2% FBS. Cells were infected at a multiplicity of infection (MOI) of 0.01 pfu/cell with 100 μ l of inoculum to ensure low rates of coinfection and complementation. Cells were allowed to adsorb virus for one hour with occasional rocking at either 37°C (Vero, DF1, A549) or 28°C (CxT, Vero). Wells were then washed three times with Hank's balanced salt solution (BA-1) to eliminate any remaining virus in the supernatant. One-hundred microliters of viral supernatant was harvested at 24-hour time points up to 5 days post-infection and placed in BA-1 containing 20% FBS for storage at -80°C. Samples were then plaque titrated. All growth curves assays were performed in triplicate and plaque titrated in duplicate. Full genome sequencing of output viruses were performed as previously described using overlapping amplicons pooled and sequenced on the Illumina MiSeq platform at the Advanced Genomic Technologies Core.⁹ Using Geneious Prime, Illumina reads were assembled to reference genome DQ164190, and minority mutations >2% were identified with a minimum coverage of 100x to assess reversion proportions.

Structural modeling

All structures were modeled in PyMOL⁴⁸ and structures were attained from the Protein Data Base (PDB). Initial modeling was performed on the WNV Kunjin helicase (PDB code 2QEQ),⁴⁹ where the proline located at position 319 was mutated into a leucine using the mutagenesis wizard. Positioning of the mutation was compared to HCV helicases, which have been crystallized in other conformations. Structures were superimposed to ensure similarity by WNV helicase and HCV helicase. The mutation was located at position 325. Subsequent modeling was performed on the HCV helicases to determine the mutation's effect on conformational changes. Two HCV helicases, PDB code 1A1V⁵⁰ and 5E4F,⁵¹ were used to visualize the conformational change of the helicase using the 'morph' command. The displayed RNA originated in 1A1V, while the bound ADP is from structure 5E4F.

Vector competence

Infection, dissemination, and transmission of WNV WTic and WNV NS3 P319L was evaluated after blood feeding to determine differences in vector competence.⁴⁴ Seven-day old female colony *Cx. pipiens* were sugar starved for 48 hours then offered a 1:10 mixture of the appropriate virus: chicken blood (Colorado Serum Company) at a concentration of 5×10^7 pfu/ml of each virus. Mosquitoes were offered infectious blood via Hemotek feeder (Discovery Workshops) for one hour. Fed and unfed mosquitoes were cold sorted in a chamber containing CO₂. Fully engorged mosquitoes were housed in gallon containers.

The experimental group had a total of at least 150 fed mosquitoes divided into 3 cups for each timepoint. On days 7, 14 and 21 post feeding, 50 mosquitoes per experimental group were incapacitated, their legs removed and placed in mosquito diluent consisting of 20% FBS, 50 micrograms of streptomycin per milliliter, 50 units of penicillin and 2.5 micrograms of amphotericin B per milliliter in PBS. Mosquitoes then had their proboscis placed in a capillary tube containing FBS plus 50% sucrose for 30 minutes to collect saliva. Bodies were then removed and stored in mosquito diluent and capillaries were ejected into 300 microliters mosquito diluent. Bodies, legs and saliva were tested for virus using qRT-PCR and/or plaque assay as described above to indicate infection, dissemination, and transmission, respectively.

Mosquito life-history traits

Mosquito life-history traits were assessed as in.³¹ Seven-day old adult female *Cx. pipiens* were starved and fed as in the vector competence assay. A total of four groups, each consisting of ~75 fed female mosquitoes and approximately 5 males were stored in gallon containers. The groups consisted of WNV WTic fed, WNV NS3 P319L fed, and a negative control group fed noninfectious blood. Mosquitoes were checked daily for mortality, which was noted. Dead mosquitoes were aspirated from gallon containers, their legs removed and both bodies and legs stored separately in mosquito diluent. Mosquitoes were offered a noninfectious bloodmeal at intervals of 7 days after infection and fed sugar on cotton pads *ad libitum*. Fed and unfed mosquitoes were counted after each bloodmeal to determine feeding rate. Egg cups were placed into each container 4 days after each blood meal and removed 2 days later, at which time rafts were counted to determine fecundity. All mosquito bodies and legs were tested via plaque titration for the presence of virus.

Avian competence

Specific-pathogen-free chicks were obtained from Charles River Laboratories (New York, NY). Chicks (3 days-old) were separated into two experimental groups of eight birds each and one control group of four birds. Experimental groups were inoculated subcutaneously in the cervical region with 10^3 pfu of WNV WTic or WNV NS3 P319L in 0.1 mL animal diluent (phosphate buffered saline with 1% fetal bovine serum). Control birds were inoculated with 0.1 mL animal diluent. For each group, one half of the number of birds were bled days 1, 3, 5 post-inoculation and one half of the birds were bled days 2, 4, and 6 post-infection. Birds were bled by lancing the brachial vein using a 27G needle and collecting blood into a 75MM heparinized capillary tube (Drummond Scientific Company, Broomall, PA). At day 7 post-inoculation, birds were euthanized using CO₂ and tissues collected (brain, kidney). Viremia was measured using plaque assay as previously described. All procedures for experimental infection of chicks were approved by IACUC at Wadsworth Center, New York State Department of Health (21-355).

Construction of WNV NS3 bacterial expression plasmids

The WNV NS3 gene was cloned into the pSUMO bacterial expression plasmid using a similar procedure as described for poliovirus RdRp (3D gene).⁵² This system allows for the production of SUMO fusion proteins containing an amino-terminal hexahistidine tag fused to SUMO that can be purified by nickel nitriloacetic acid (Ni-NTA) chromatography and subsequently processed by the SUMO protease, ubiquitin-like-specific protease-1 (Ulp1). The WNV NS3 coding region was amplified by PCR and the PCR product was gel purified and cloned into the pSUMO plasmid using BsaI and Sall sites. The final construct (pSUMO-WNV NS3) was confirmed by sequencing at the Pennsylvania State University's Nucleic Acid Facility.

The P319L mutation was introduced via mutagenic high fidelity PCR (Q5 High Fidelity, New England Biolabs) followed by Zymo DNA Clean and Concentrator (New England Biolabs), then fragments were assembled (NEBuilder HiFi DNA assembly) and transformed into *E. coli* DH5 alpha cells. Colonies evidencing kanamycin resistance were screened for mutation. An SmaI site was inserted to determine successful mutation of the plasmid. Extraction of plasmid DNA was performed using ZymoPURE prep kit following the manufacturer's instructions. Whole genome sequencing was performed as above to confirm genotype.

Expression and purification of WNV NS3

E. coli Rosetta (DE3) cells were transformed with the pSUMO-WNV-NS3 plasmid for protein expression. Rosetta (DE3) cells containing the pSUMO-WNV-NS3 plasmid were grown in 100 mL of media (NZCYM) supplemented with 25 µg/mL kanamycin (K25) and 20 µg/mL chloramphenicol (C20) at 37°C until an OD₆₀₀ of 1.0 was reached. This culture was then used to inoculate 1 L of K75, C60-supplemented

ZYP-5052 auto-induction media,⁵³ to an OD₆₀₀= 0.1. The cells were grown at 37°C to an OD₆₀₀ of 0.8 to 1.0, cooled to 20°C and then grown for 24 h. Typically, after 24 h at 20°C the OD₆₀₀ reached ~10-15. Cells were harvested by centrifugation (6000 x g, 10 min) and the cell pellet was washed once in 200 mL of TE buffer (10 mM Tris, 1 mM EDTA), centrifuged again, and the cell paste weighed. The cells were then frozen and stored at -80°C until used. Frozen cells were thawed and suspended in lysis buffer (20 mM Potassium Phosphate pH 8.0, 20% glycerol, 5 mM Imidazole, 500 mM NaCl, 5 mM BME, 1.4 ug/ml Pepstatin A, and 1.0 ug/ml Leupeptin), 5 mL/g cell pellet. The cell suspension was lysed by passing through a French press (SLM-AMINCO) at 15,000 psi. After lysis, phenylmethylsulfonylfluoride (PMSF) and NP-40 were added to a final concentration of 1 mM and 0.1% (v/v), respectively. While stirring the lysate, polyethylenimine (PEI) was slowly added to a final concentration of 0.25% (v/v) and then centrifuged at 75,000 x g for 30 min at 4°C. The PEI supernatant was decanted to a fresh beaker, and while stirring, pulverized ammonium sulfate was slowly added to 40% (w/v) saturation. This supernatant was stirred for 30 min after the last addition of ammonium sulfate, and centrifuged at 75,000 x g for 30 min at 4°C. The supernatant was decanted, and the pellet was suspended in buffer B (25 mM HEPES, pH 7.5, 500 mM NaCl, 5 mM BME, 20% glycerol) with 5 mM imidazole. The resuspended ammonium sulfate pellet was loaded onto a Ni-NTA column (Qiagen) at a flow rate of 1 mL/min (approximately 1 mL bed volume/100 mg total protein) equilibrated with buffer B. After loading, the column was washed with twenty column volumes of buffer B containing 5 mM imidazole and five column volumes of buffer B containing 50 mM imidazole. Protein was eluted from the Ni-NTA column with buffer B containing 500 mM imidazole. Fractions were collected and assayed for purity by SDS-PAGE. Ulp1 (1 µg per 10 mg SUMO fusion protein) was added to the purified protein at 4°C to cleave the SUMO-NS3 fusion protein. Purified protein was aliquoted and frozen at -80°C until use.

NS3 ATPase activity and quantification

Reactions were performed at 37°C and 28°C. Reactions contained 20 mM MOPS pH 7.0, 50 mM NaCl, 1 mM TCEP, 0.5 mM MgCl₂, 2 mM ATP and 0.1 µCi/µL [α -³²P]-ATP. Reactions were initiated by the addition of NS3 (300 nM final). Reactions were quenched at various times by addition of EDTA to 100 mM. NS3 was diluted immediately prior to use in buffer B. The volume of enzyme added to any reaction was always less than or equal to one-tenth the total volume. Quenched reactions were spotted onto polyethylenimine-cellulose TLC plates (EM Science). TLC plates were developed in 0.3 M potassium phosphate, pH 7.0, dried, exposed to a PhosphorImager screen, visualized by using a TyphoonImager (Cytiva) and quantified by using ImageQuant TL software (Cytiva).

QUANTIFICATION AND STATISTICAL ANALYSIS

Statistical analyses performed include unpaired and paired t-tests, chi-squared tests, log rank tests, Fisher's exact tests, and linear regression analyses. All statistics were performed using GraphPad Prism 7.05. Statistical details can be found in the figure legends and results.